

An ultrasmall wavelength-selective channel drop switch using a nanomechanical photonic crystal nanocavity

著者	Kanamori Yoshiaki, Takahashi Kazunori, Hane Kazuhiro
journal or publication title	Applied Physics Letters
volume	95
number	17
page range	171911
year	2009
URL	http://hdl.handle.net/10097/51575

doi: 10.1063/1.3254247

An ultrasmall wavelength-selective channel drop switch using a nanomechanical photonic crystal nanocavity

Yoshiaki Kanamori,^{a)} Kazunori Takahashi, and Kazuhiro Hane
 Department of Nanomechanics, Tohoku University, Sendai 980-8579, Japan

(Received 23 July 2009; accepted 6 October 2009; published online 30 October 2009)

We propose a nanomechanical channel drop switch by controlling the submicron distance between a nanocavity and photonic crystal (PC) waveguide with an ultrasmall electrostatic comb actuator. Light propagating in the PC waveguide is coupled with a nanocavity and emitted as a drop signal under a resonant condition. The proposed switch has been fabricated by silicon micromachining. The drop efficiency has been controlled by 12.5 dB and gap change of 600 nm. © 2009 American Institute of Physics. [doi:10.1063/1.3254247]

Photonic crystals (PCs),¹⁻⁷ which can confine light in micro/nanoregions, have great potential as integrated optical circuits and highly efficient photonic devices. Nanocavities^{3-5,7} are point defects in PCs that can strongly confine light in a region smaller than an optical wavelength. It has also been reported that nanocavities are useful for ultrasmall add/drop filters.³⁻⁵ Similar to microring resonators, which have been extensively studied for wavelength division multiplex (WDM) optical telecommunication,^{8,9} tuning of nanocavities is also promising for functional devices. Tuning of nanocavities using a thermorefractive effect⁵ and nanoprobe interaction⁶ has been proposed. Very fast modulation of a nanocavity using the refractive-index change by two-photon absorption has also been demonstrated.⁷ On the other hand, several variable PC devices integrated with microelectromechanical actuators in order to obtain a large tuning range have recently been reported.¹⁰⁻¹⁴ Although few devices have actually been fabricated, Lee *et al.*¹⁰ installed a one-dimensional PC filter with a microactuator in a waveguide switch. Kanamori *et al.*¹³ also fabricated a movable PC filter to control guided resonance using microelectromechanical actuators. Recently, Huang *et al.*¹⁴ demonstrated a high-speed nanoelectromechanical tunable laser by monolithically integrating a one-dimensional PC filter as a movable top mirror in a vertical-cavity surface-emitting laser.

In this letter, we propose a channel drop switch integrated with an ultrasmall electrostatic comb actuator based on nanomechanical tuning of a PC nanocavity. By switching the coupling efficiency, an ultrasmall channel drop filter, which can control the path of the light wave, is realized.

The proposed device consists of a PC waveguide and a movable PC nanocavity as schematically illustrated in Fig. 1(a). The PC waveguide consists of an edge waveguide of a PC slab, in which the propagating wave is confined on the left side by a PC slab, as shown in Fig. 1(a), while on the right side, it is confined by a low index surrounding air. Also the air gap works as a slotted PC waveguide,^{15,16} which alters dispersion of the PC waveguide. The nanocavity is a PC defect located in a movable PC slab. The air gap between them can be adjusted by translation of the movable PC slab. The light wave propagating in the PC waveguide can interact with the nanocavity under its resonant condition, and thus it is dropped from the PC waveguide to the nanocavity if the

coupling between them is large. The nanocavity emits the dropped light in the direction vertical to the PC slab. If the gap is closed, the optical configuration is similar to the reported nanocavity add/drop filter.^{3,4} When a gap is introduced, the position of the fundamental waveguide mode in photonic bandgap changes because of the existence of the slotted mode. Also this waveguide is no longer single-mode. The band structure is also altered by a change in the gap, so we need to consider carefully the slotted mode in the design. At a large gap, the light wave propagates in the PC waveguide without interacting with the nanocavity. The calculated electrical fields at the resonant wavelength of the nanocavity are presented in Fig. 1(b). The calculations were carried out using the finite difference time domain (FDTD) method. As an example, the nanocavity was designed to consist of three linear missing air holes in the third row of the PC slab, and the PC waveguide consisted of one row of missing air holes. The PC air hole diameter, lattice constant, and thickness were 240, 420, and 260 nm, respectively. As can be seen in Fig. 1(b), little light is coupled with the nanocavity at a gap of 500 nm. By decreasing the gap, the light wave coupled with the nanocavity increases at gaps of 250 and 50 nm, as shown in Fig. 1(b).

The drop efficiency, i.e., the ratio of emitted power from the nanocavity, which is created in the fourth row of the PC

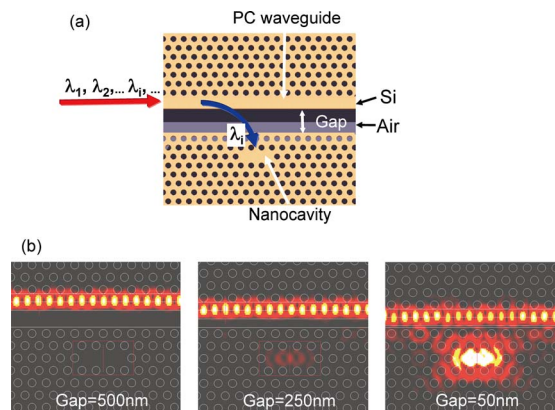


FIG. 1. (Color online) A wavelength-selective channel drop switch with a PC waveguide and a movable PC nanocavity. (a) Schematic of the proposed device. (b) Calculated electrical fields at the resonant wavelength of the nanocavity depending on the gap. A continuous wave at a resonant wavelength of 1.5340 μm was assumed as a light source.

^{a)}Electronic mail: kanamori@hane.mech.tohoku.ac.jp.

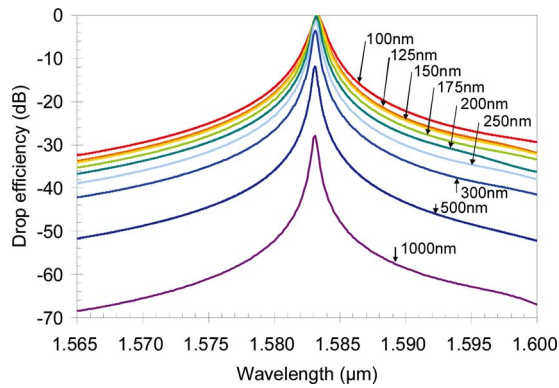


FIG. 2. (Color online) Calculated drop efficiency from the nanocavity as a function of wavelength with air gap as a parameter. The numerical value indicating each curve shows the gap.

slab, to the input power is numerically calculated as a function of wavelength with air gap as a parameter. The drop efficiency normalized by the maximum value obtained at the gap of 175 nm and at a resonant wavelength of $1.5832 \mu\text{m}$ is shown in Fig. 2. The maximum drop efficiency is obtained under the critical coupling condition, which is not equal to the physical contact in this simulation, similar to the conventional waveguide coupler. With an increase in the gap larger than that of the critical coupling, the drop efficiency exponentially decreases. At a gap of 1000 nm, the resonant peak decreases by 28 dB when compared with that under the critical condition. Therefore, with a gap change smaller than $1 \mu\text{m}$, the coupling between the PC waveguide and nanocavity can be greatly controlled.

In order to achieve the above conceptual mechanism supported by the calculated results, we designed a nanomechanical structure for the channel drop PC switch with an ultrasmall actuator, as shown in Fig. 3(a). In addition to the PC waveguide and movable PC nanocavity, two suspended Si waveguides are connected to the PC waveguide as input and output ports. The actuator consists of a fixed comb and

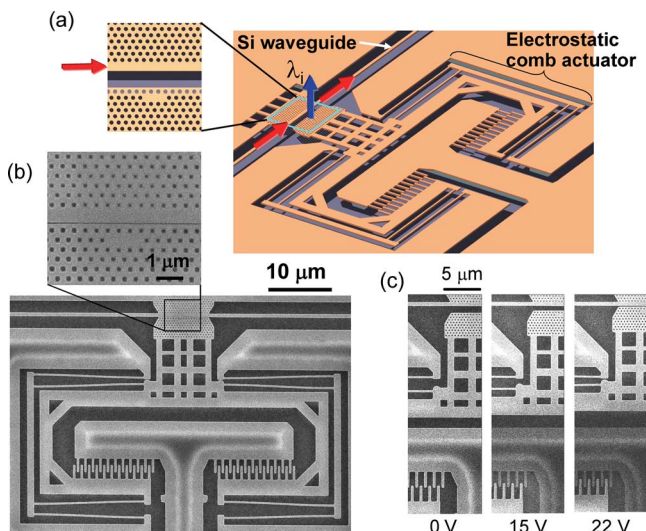


FIG. 3. (Color online) Nanomechanical channel drop PC switch with an ultrasmall actuator. (a) Schematic of a nanomechanical channel drop PC switch. (b) Scanning electron micrograph of the fabricated device fabricated by etching a $2\text{-}\mu\text{m}$ -thick SiO_2 layer under the movable structure. (c) Scanning electron micrographs of the device obtained at voltages of 0, 15, and 22 V applied to the actuator.

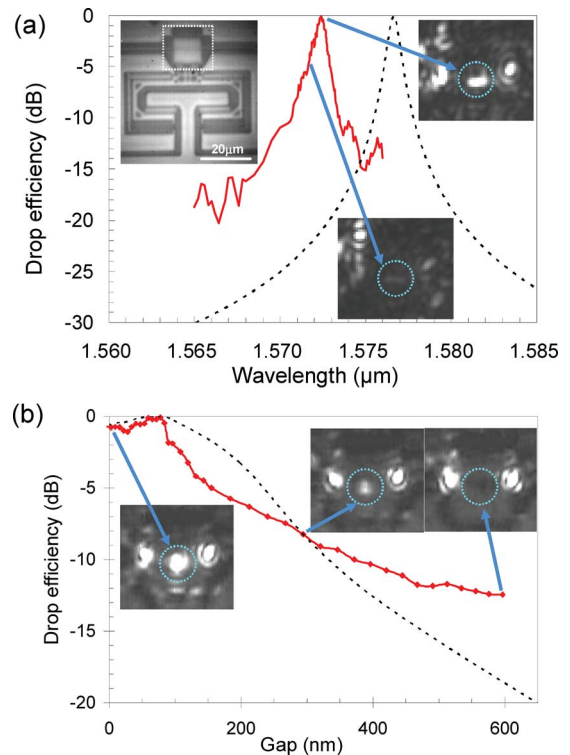


FIG. 4. (Color online) Optical characteristic of the nanomechanical channel drop PC switch. (a) Drop efficiency measured (solid curve) and calculated (dotted curve) as a function of incident wavelength when the PC nanocavity slab comes into contact with the PC waveguide. The calculations were carried out using the FDTD method with the Si refractive index of 3.4. The upper right and lower insets show infrared optical micrographs of the PC nanocavity slab obtained at wavelengths of 1.5724 and $1.5717 \mu\text{m}$, respectively. The imaged region of the PC nanocavity slab is indicated by the dotted area in upper left inset, which shows a micrograph of the whole view of the fabricated device. (b) Drop efficiency measured (solid curve) and calculated (dotted curve) as a function of air gap between the PC waveguide and the PC nanocavity slab at the resonant wavelength of $1.5724 \mu\text{m}$. The insets show infrared optical micrographs of the PC nanocavity slab.

a movable comb with 200-nm-wide, 260-nm-thick, and $1.5\text{-}\mu\text{m}$ -long comb fingers.¹⁷ The spring constant of the actuator is 0.11 N/m , consisting of 250-nm-wide double-folded springs. By applying voltage to the comb electrodes, the lateral position of the nanocavity is controlled within $1 \mu\text{m}$. Figure 3(b) shows scanning electron micrographs of the fabricated device. The device was fabricated from a silicon-on-insulator wafer, which is compatible with conventional PC slab fabrications. A nanocavity consisting of three missing air holes and the self-suspended actuator has been fabricated well. Displacement of the actuator was observed by a scanning electron microscope with increase in the driving voltage applied to the comb electrodes, as shown in Fig. 3(c). By increasing the voltage to the actuator, the gap is changed precisely. At the voltage of 22 V, the actuator moved by $1 \mu\text{m}$. The switching frequency of the nanomechanical device was commonly limited by the mechanical resonant frequency of the moving part. A sinusoidal voltage with amplitude of 1.1 V was applied to the actuator, and the vibration amplitude of the movable PC nanocavity slab was measured as a function of frequency. A resonant oscillation was observed at the frequency of 132 kHz with width of 0.5 kHz under a vacuum condition. The measured resonant frequency was close to the calculated value of 129 kHz.

Figure 4(a) shows the drop efficiency as a function of

incident wavelength when the PC nanocavity slab comes into contact with the PC waveguide. The results of measurements and calculations are shown by solid and dotted curves, respectively, after normalization by their maximum values. The measured drop efficiency increases by about 18 dB from the off-resonant condition around $1.565 \mu\text{m}$, and it becomes maximum at the resonant wavelength of $1.5724 \mu\text{m}$ and decreases sharply with further increase in wavelength. The bandwidth is 0.90 nm. The infrared optical micrographs of the PC nanocavity slab are shown in the insets of Fig. 4(a). At the resonant wavelength of $1.5724 \mu\text{m}$, a bright light spot is observed at the center of the image, as shown by the dotted circles. The bright spot corresponds to the light emitted from the nanocavity. On the other hand, at the off-resonant wavelength of $1.5717 \mu\text{m}$, the bright spot disappears, as shown in the corresponding inset of Fig. 4(a). In the calculations, the resonant wavelength and bandwidth are $1.5766 \mu\text{m}$ and 0.75 nm, respectively. The results of calculations roughly explain the measured drop efficiency as a function of wavelength. Figure 4(b) shows the drop efficiency as a function of the air gap between the PC waveguide and the PC nanocavity slab. The results of measurements and calculations are shown by solid and dotted curves, respectively, after normalization by their maximum values. The drop efficiency increases with a decrease in the gap from 600 nm. At a gap of approximately 80 nm, the drop efficiency becomes maximum, which corresponds to the critical coupling between the nanocavity and the PC waveguide. With further decrease in the gap, the efficiency decreases slightly. The results of measurements show that drop efficiency is controlled by 12.5 dB by gap change of 600 nm. With a decrease in the gap, the light spot observed at the position of the nanocavity denoted by the dotted circle becomes brighter, as shown in the insets. The calculated drop efficiency explains the measured drop efficiency as a function of air gap. The calculated gap for the critical coupling is about 75 nm, which also agrees with the measured value.

Under the critical coupling condition at the wavelength of $1.5724 \mu\text{m}$, the absolute value of drop efficiency was obtained from the measured spot intensities to be -6.1 dB , corresponding to 24.56% of the input waveguide intensity. According to a report on a nanocavity drop filter,⁴ the theoretical maximum drop efficiency is calculated to be 50% by summing up the emissions upward and downward from the

nanocavity. Therefore, the measured drop efficiency is about half of the theoretical maximum value.

In conclusion, we demonstrated a wavelength-selective drop switch by controlling the light wave coupling between a nanocavity and PC waveguide with an ultrasmall electrostatic comb actuator. The drop efficiency from the nanocavity was greatly varied by changing the submicron air gap. Multi-channel-selectable add/drop switches can be realized by connecting in series movable PC nanocavities with different resonant wavelengths, which can be key components to develop ultrasmall tunable PC circuits for WDM optical communication systems.

This work was partially supported by JSPS (Grant Nos. 17068002 and 19106007). The authors thank Professor T. Baba, Yokohama National University, for helpful suggestions.

- ¹S. J. McNab, N. Moll, and Y. A. Vlasov, *Opt. Express* **11**, 2927 (2003).
- ²T. N. Oder, K. H. Kim, J. Y. Lin, and H. X. Jiang, *Appl. Phys. Lett.* **84**, 466 (2004).
- ³Y. Akahane, M. Mochizuki, T. Asano, Y. Tanaka, and S. Noda, *Appl. Phys. Lett.* **82**, 1341 (2003).
- ⁴A. Chutinan, M. Mochizuki, M. Imada, and S. Noda, *Appl. Phys. Lett.* **79**, 2690 (2001).
- ⁵T. Asano, W. Kunishi, M. Nakamura, B. S. Song, and S. Noda, *Electron. Lett.* **41**, 37 (2005).
- ⁶S. Mujumdar, A. F. Koenderink, T. Suenner, B. C. Buchler, M. Kamp, A. Forchel, and V. Sandoghdar, *Opt. Express* **15**, 17214 (2007).
- ⁷T. Tanabe, M. Notomi, S. Mitsugi, A. Shinya, and E. Kuramochi, *Appl. Phys. Lett.* **87**, 151112 (2005).
- ⁸Y. Goebuchi, T. Kato, and Y. Kokubun, *IEEE Photonics Technol. Lett.* **18**, 538 (2006).
- ⁹K. Takahashi, Y. Kanamori, Y. Kokubun, and K. Hane, *Opt. Express* **16**, 14421 (2008).
- ¹⁰M.-C. M. Lee, D. Hah, E. K. Lau, H. Toshiyoshi, and M. Wu, *IEEE Photonics Technol. Lett.* **18**, 358 (2006).
- ¹¹K.-I. Umemori, Y. Kanamori, and K. Hane, *Appl. Phys. Lett.* **89**, 021102 (2006).
- ¹²S. Iwamoto, S. Ishida, Y. Arakawa, M. Tokushima, A. Gomyo, H. Yamada, A. Higo, H. Toshiyoshi, and H. Fujita, *Appl. Phys. Lett.* **88**, 011104 (2006).
- ¹³Y. Kanamori, T. Kitani, and K. Hane, *Appl. Phys. Lett.* **90**, 031911 (2007).
- ¹⁴M. C. Y. Huang, Y. Zhou, and C. J. Chang-Hasnain, *Nat. Photonics* **2**, 180 (2008).
- ¹⁵V. R. Almeida, Q. Xu, C. A. Barrios, and M. Lipson, *Opt. Lett.* **29**, 1209 (2004).
- ¹⁶A. Di Falco, L. O'Faolain, and T. F. Krauss, *Appl. Phys. Lett.* **92**, 083501 (2008).
- ¹⁷K. Takahashi, E. Bulgan, Y. Kanamori, and K. Hane, *IEEE Trans. Ind. Electron.* **56**, 991 (2009).